Appl Microbiol Biotechnol (2017) 101:8499–8516
https://doi.org/10.1007/s00253-017-8572-2

GENOMICS, TRANSCRIPTOMICS, PROTEOMICS

Copper and cerium-regulated gene expression in *Methylosinus trichosporium* OB3b

Wenyu Gu[1] · **Jeremy D. Semrau**[1]

Received: 12 June 2017 / Revised: 25 September 2017 / Accepted: 2 October 2017 / Published online: 14 October 2017

Abstract In aerobic methanotrophs, copper and cerium control the expression and activity of different forms of methane monooxygenase and methanol dehydrogenase, respectively. To exploit methanotrophy for the valorization of methane, it is crucial to determine if these metals exert more global control on gene expression in methanotrophs. Using RNA-Seq analysis we compared the transcriptome of *Methylosinus trichosporium* OB3b grown in the presence of varying amounts of copper and cerium. When copper was added in the absence of cerium, expression of genes encoding for both soluble and particulate methane monooxygenases varied as expected. Genes encoding for copper uptake, storage, and efflux also increased, indicating that methanotrophs must carefully control copper homeostasis. When cerium was added in the absence of copper, expression of genes encoding for alternative methanol dehydrogenases varied as expected, but few other genes were found to have differential expression. When cerium concentrations were varied in the presence of copper, few genes were found to be either up- or downregulated, indicating that copper over rules any regulation by cerium. When copper was increased in the presence of cerium, however, many genes were upregulated, most notably multiple steps of the central methane oxidation pathway, the serine cycle, and the ethylmalonyl-CoA pathway. Many genes were also downregulated, including those encoding for nitrogenase and hydrogenase. Collectively, these data suggest that copper plays a larger role in regulating gene expression in methanotrophs, but that significant changes occur when both copper and cerium are present.

Keywords Methanotrophs · Copper · Cerium · RNA-Seq · RT-qPCR

Introduction

Aerobic methane-oxidizing bacteria—methanotrophs—thrive wherever methane-air interfaces develop, including in freshwater and marine sediments, bogs, forest, and agricultural soils as well as aquifers (Hanson and Hanson 1996; Op den Camp et al. 2009; Semrau et al. 2010). These microbes play a critical role in the global carbon cycle through the conversion of methane to biomass and carbon dioxide and have received a great deal of attention for their potential in producing a wide range of valuable products from the inexpensive and widely available carbon source methane (Kalyuzhnaya et al. 2015; Khmelenina et al. 2015; Semrau et al. 2010; Strong et al. 2015).

The activity of methanotrophs, however, is strongly affected by a number of environmental parameters, especially the bioavailability of copper. Some methanotrophs have a well-known "copper-switch" where the type and activity of methane monooxygenase responsible for the initial oxidation of methane to methanol responds significantly to the availability of copper (Nielsen et al. 1996, 1997; Stanley et al. 1983). That is, when grown at low copper conditions, a cytoplasmic or soluble methane monooxygenase (sMMO) is expressed. As the copper concentration in the medium increases, expression of sMMO decreases and expression and activity of a membrane-bound or particulate methane monooxygenase (pMMO) increases (Choi et al. 2003; Semrau et al. 2013). This response to copper is important for the application of methanotrophs as the sMMO

Electronic supplementary material The online version of this article (https://doi.org/10.1007/s00253-017-8572-2) contains supplementary material, which is available to authorized users.

✉ Jeremy D. Semrau
jsemrau@umich.edu

[1] Department of Civil and Environmental Engineering, University of Michigan, Ann Arbor, MI 48109-2125, USA

and pMMO have very different substrate ranges and kinetics. The sMMO has a very broad substrate range and so has more potential in biocatalysis applications, but also has a poor affinity for methane, limiting its use for scavenging methane at low concentrations (Kalyuzhnaya et al. 2015; Lee et al. 2006; Semrau et al. 2010; Trotsenko and Murrell 2008). pMMO, conversely, has relatively low turnover but greater affinity for methane (Lee et al. 2006) and so is likely to be more useful for control of methane emissions (Yoon et al. 2009).

More recently, rare earth elements (REEs) such as cerium have been shown to have a major effect on methanotrophs (Keltjens et al. 2014; Pol et al. 2014). That is, REEs strongly regulate the activity and expression of alternative methanol dehydrogenases (MeDH) that oxidize methanol, signifying that a "REE-switch" also exists (Chu and Lidstrom 2016; Farhan UI Haque et al. 2015a; Gu et al. 2016; Hibi et al. 2011; Nakagawa et al. 2012). Two different forms of MeDH have been found in most but not all methanotrophs (Pol et al. 2014; Vekeman et al. 2016). One form is a heterotetrameric protein ($\alpha_2\beta_2$) with two 66-kDa (α) subunits (MxaF) and two 8.5 kDa (β) subunits (MxaI). In this canonical MeDH (Mxa-MeDH), calcium is in the active site and is coordinated with pyrroloquinoline quinone, or PQQ (Anthony and Williams 2003; Goodwin and Anthony 1998; Williams et al. 2005). A homolog to the large subunit, XoxF, is also present that encodes for another PQQ-dependent methanol dehydrogenase (Xox-MeDH) (Skovran et al. 2011; Wu et al. 2015). Xox-MeDH is a homodimer of XoxF (Schmidt et al. 2010; Pol et al. 2014) sometimes associated with MxaI (Wu et al. 2015). Xox-MeDH has a rare earth element in its active site (Pol et al. 2014), and it has been shown that expression of Mxa-MeDH vs. Xox-MeDH depends on the availability of REEs. In the absence of REEs, little expression of Xox-MeDH is observed, but such expression increases significantly when REEs are added (e.g., Chu and Lidstrom 2016; Farhan HI Haque et al. 2015a; Gu et al. 2016; Vu et al. 2016; Wehrmann, et al. 2017).

What is not clear, however, is if copper and/or cerium exert more global control over gene expression in methanotrophs. These metals clearly control expression of enzymes mediating the oxidation of methane and methanol—two key steps in the central pathway of methane oxidation—but do they regulate expression of genes in other metabolic pathways? Here, we describe the effect of different concentrations of copper and/or cerium on the transcriptome of *Methylosinus trichosporium* OB3b using RNA sequencing (RNA-Seq) and RT-qPCR.

Materials and methods

Culture conditions

M. trichosporium OB3b (NCIMB 11131; VKM B-2117; Whittenbury et al. 1970) was grown on nitrate mineral salts (NMS) medium (Whittenbury et al. 1970) at 30 °C in 250-ml side-arm Erlenmeyer flasks sealed with rubber stoppers. The flasks were shaken at 200 rpm in dark. CH_4 was added at a methane-to-air ratio of 1:2. To investigate the effect of copper and cerium on the transcriptome of *M. trichosporium* OB3b, this strain was grown under four different conditions using side-arm flasks to noninvasively monitor growth: 0 μM copper + 0 μM cerium, 0 μM copper + 25 μM cerium, 10 μM copper + 0 μM cerium, and 10 μM copper + 25 μM cerium. These concentrations were chosen as similar values have been often used earlier to examine the effect of copper and rare earth elements on gene expression in methylotrophs (e.g., Chu and Lidstrom 2016; Farhan Ul Haque et al. 2015a; Gu et al. 2016; Vu et al. 2016). All conditions had triplicate biological replicates. Copper and cerium were added as $CuCl_2$ and $CeCl_3$, respectively. Growth of these cultures was monitored via OD_{600} using a Genesys 20 Visible spectrophotometer (Spectronic Unicam, Waltham, MA, USA) at 4–12 h intervals. The growth rates of *M. trichosporium* OB3b when grown under these four conditions were not significantly different, as documented earlier (Farhan Ul Haque et al. 2015a) and observed again in this study (data not shown). It should be noted that a substantial fraction (70–90%) of added cerium formed insoluble precipitate(s) in standard NMS growth medium that could be removed via centrifugation at 5000×*g* for 10 min (data not shown). Variable amounts of copper and iron (10–15%) also co-precipitated with the insoluble cerium compound(s) (data not shown). It is unknown if any fraction of these precipitated metals is bioavailable (e.g., through the production of siderophores or chalkophores).

Total RNA isolation and purification

After cultures entered the mid-exponential phase (OD_{600} of ~ 0.3), total RNAs were isolated using the method described before (Gu et al. 2016; Semrau et al. 2013). Briefly, 20 ml from each flask was first mixed with 2.5 ml stop solution [5% buffer equilibrated phenol (pH 7.3) in ethanol] to stop synthesis of new mRNA and then centrifuged at 4000*g* for 10 min at 4 °C. The cell pellets were then resuspended in 0.75 ml of extraction buffer [100 mM Tris-HCl (pH 8.0), 1.5 M NaCl, 1% (*w*/*v*) hexadecyltrimethylammonium bromide (CTAB)] and subjected to lysis by bead beating using 0.5 g 0.1-mm zirconia-silica beads at 4800 rpm for 1 min (Biospec Products, Bartlesville, OK, USA) in the presence of 35 μl 20% SDS, 35 μl 20% laurylsarcosine, and 750 μl phenol-chloroform-isoamylic alcohol (25:24:1). The samples were then centrifuged at 18,000 *g* for 5 min at 4 °C and the upper aqueous phase was transferred to a new tube and mixed with an equal volume of chloroform-isoamylic alcohol (24:1). The mixture was centrifuged again and the upper aqueous phase containing RNA was precipitated in $MgCl_2$, sodium acetate, and isopropanol overnight at − 80 °C.

RNA was recovered the next day by centrifugation at 18,000*g* for 30 min at 4 °C and washed by 75% ethanol. DNA was removed by RNase-free DNase (Qiagen, Hilden, Germany) through at least two treatments, followed by purification using a Zymo RNA Clean & Concentrator kit (Zymo Research, Irvine, CA, USA) following the manufacturer's instructions. Removal of all traces of DNA was confirmed by the absence of a 16S rRNA PCR product in reactions using 2 μl of RNA template and 32 PCR cycles. RNA concentrations were estimated by using an ND-1000 spectrophotometer (NanoDrop Technologies Inc., Wilmington, DE, USA).

RNA sequencing

Following the purification of total RNA, ribosomal RNA was removed using the RiboZero kit for Gram-negative bacteria (Illumina, San Diego, CA, USA). The qualities of the samples were checked by Agilent bioanalyzer (Santa Clara, CA, USA). mRNA-Seq libraries were then prepared by University of Michigan DNA Sequencing Core (http://seqcore.brcf.med.umich.edu) and sequenced in one lane using Illumina (San Diego, CA, USA) HiSeq4000 SE 50.

Differential expression analysis

The raw reads obtained from the sequencing core were trimmed using Sickle 1.33 (Joshi and Fass 2011) with default parameters for single-end reads and then aligned to the *M. trichosporium* OB3b genome (WGS ADVE02) downloaded from Genoscope (https://www.genoscope.cns.fr/agc/microscope/home/index.php) using the Burrows-Wheeler alignment tool (BWA) backpack 0.7.12 (Li and Durbin 2009) with default parameters. The quality of sequences was checked at each step by FastQC v0.11.5 (Andrews 2010). The resulting sequence alignment/map (SAM) files were then sorted using SAMtools-1.3.1 (Li et al. 2009). Reads were assigned to features and counted using HTSeq 0.6.1p1 with "intersection-nonempty" and "–a = 0" mode (Anders et al. 2015) based on annotation downloaded from Genoscope. Differential expression was analyzed by DESeq2 v1.12.4 (Anders and Huber 2010) in R v3.3.0. Sequences were also analyzed by bowtie2 (v2.2.9) (Langmead and Salzberg 2012) for alignment and voom/limma (v3.28.21) (Law et al. 2014) with default parameters for differential expression. Results obtained from both pipelines were comparable and the results obtained by DESeq2 method presented here. Genes were considered to be differentially expressed if a Benjamini-Hochberg-adjusted p value $< 1 \times 10^{-3}$ and $|\log_2|$fold change > 1.5.

Reverse transcription-quantitative polymerase chain reaction

Differential expression of selected genes was verified by RT-qPCR using the comparative C_T method (Schmittgen and Livak 2008). These were *pmoA* (encoding for the 27 kDa polypeptide of pMMO), *mmoX* (encoding for the α-subunit of sMMO hydroxylase), *xoxF12* (encoding for the 65-kDa polypeptides of Xox12-MeDH), *mxaF* (encoding for the 66-kDa polypeptide of Mxa-MeDH), *nifH* (encoding for the dinitrogenase reductase subunit), *pvdF* (responsible for synthesis of formyl hydroxamate groups in pyoverdine), and *mbnA* (encoding for the polypeptide precursor of methanobactin). Three genes were used as internal references—*rrs* (16S rRNA), *clpX* (a subunit of a ClpX-ClpP ATP-dependent serine protease), and *yjg* (a permease of the YjgP/YjgQ family). These were chosen as *rrs* was found to be appropriate in previous studies Farhan Ul Haque et al. 2015a, b; Gu et al. 2016; Kalidass et al. 2015), and expression of *clpX* and *yjg* were observed to be invariant under the growth conditions described examined here, i.e., $\log_2$ expression changes < 0.05 as determined via RNA-Seq. Primer sets used for these reactions are shown in Supplementary Table S1. Calibration curves for qPCR of these genes are shown in Supplementary Fig. S1.

Sequence accession number

The transcriptomes of *M. trichosporium* OB3b grown with varying copper and cerium concentrations are available at the NCBI Gene Expression Omnibus database under accession number GSE90817.

Results

General analyses of transcriptomic samples

The quality of the collected RNA was very good (RIN ≥ 8.7 for each sample) with 23.1–42.8 × 10^6 reads per sample (Supplementary Table S2). Of these, 7.3–15.2 × 10^6 reads per sample were assigned to regions encoding for proteins. To determine the reproducibility of biological replicates, principal component analysis of the normalized logarithmic transformed read counts of each transcriptome was performed using DESeq2 (Anders and Huber 2010). High similarity was observed between triplicate biological replicates for three of the growth conditions—0 μM copper + 0 μM cerium, 0 μM copper + 25 μM cerium, and 10 μM copper + 25 μM cerium. Transcriptomes of replicates of the fourth growth condition—10 μM copper + 0 μM cerium—showed less uniformity (Fig. 1). Despite the variability in the transcriptome of *M. trichosporium* OB3b when grown with 10 μM copper +

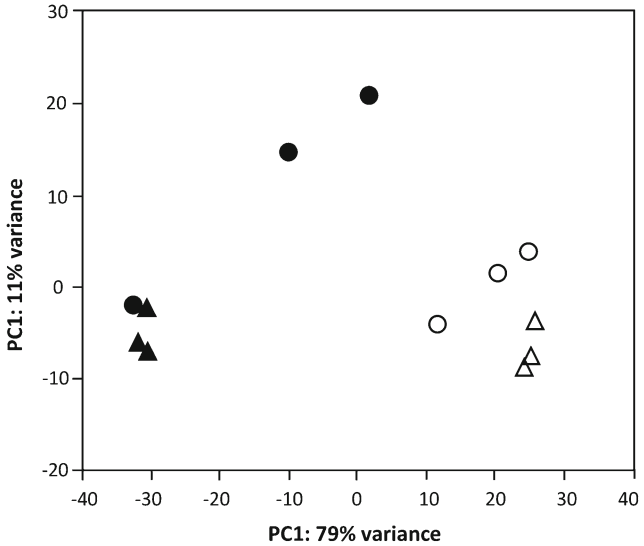

Fig. 1 Principal component analysis of collected transcriptomic sequence data. unfilled circle = 0 μM copper + 0 μM cerium, filled circle = 10 μM copper + 0 μM cerium, unfilled triangle = 0 μM copper + 25 μM cerium, filled triangle = 10 μM copper + 25 μM cerium

0 μM cerium, we could not reasonably conclude that any replicate in this condition was an outlier as (1) the coverage and sequence of these replicates were comparable and (2) the Spearman's rank correlation coefficient between these three replicates was found to be > 0.93. As such, all replicates for all conditions were included in subsequent analyses of differential gene expression.

Differentially expressed genes in the presence or absence of copper

When comparing the transcriptome of *M. trichosporium* OB3b grown with 10 μM copper + 0 μM cerium vs. 0 μM copper + 0 μM cerium, over 100 genes were found to have significant differential expression in the presence vs. absence of copper, i.e., $|\log_2|$ change ≥ 1.5 and Benjamini-Hochberg-adjusted p value ≤ 1×10^{-3}. Those genes with annotated functions are listed in Table 1, e.g., genes involved in methane oxidation, cell synthesis, metal homeostasis, and transcriptional regulation. Other genes, mostly encoding for unknown function, were also differentially regulated with respect to copper but are not shown in Table 1. Complete differential expression analyses are available in the supplementary information as Supplementary Excel File S1.

Thirty-seven genes were found to be significantly upregulated when copper was added. As expected from previous RT-qPCR assays of *pmoA* (Farhan UI Haque et al. 2015a; Kalidass et al. 2015; Semrau et al. 2013), these included genes of the *pmo* operons. Further, a gene (locus tag ADVE02_v2_12455), encoding for a recently discovered copper storage protein, Csp1, (Vita et al. 2016) was also significantly upregulated in the presence of copper but its homolog, Csp2 (locus tag ADVE02_v2_10455), did not vary with respect to copper. *cusAB*, encoding for a copper efflux system (Munson et al. 2000), was found to have increased expression in the presence vs. absence of copper. Very few other groups of genes were found to be upregulated, with the exception of genes encoding for 30S and 50S ribosomal proteins, one gene encoding for a porin, one gene encoding for a molybdate transporter (*modA*), and many genes of unknown function (Table 1; Supplementary Excel File S1).

Approximately twice as many genes (86 in total) were downregulated in the presence of copper (i.e., $\log_2$ change ≤ − 1.5 and Benjamini-Hochberg-adjusted p value ≤ 1×10^{-3}). Most notably, *mmo* genes encoding for polypeptides of the sMMO as well as *mbn* genes involved in methanobactin synthesis were downregulated. Methanobactin is a copper chelating molecule produced by some methanotrophs in copper limiting conditions for copper sequesteration (DiSpirito et al. 1998, 2016; Semrau et al. 2013). In addition, many genes encoding for TonB-dependent transporters had reduced expression in the presence of copper, as did numerous putative σ factors and proteins of unknown function (Table 1; Supplementary Excel File S1).

Differentially expressed genes in the presence or absence of cerium

Gene expression was also affected by the availability of cerium, but fewer genes showed differential expression in response to the addition of this rare earth element as compared to changes observed when copper was varied, i.e., 20 genes were upregulated and 15 downregulated in the presence vs. absence of cerium (Table 2). All genes with annotated functions are listed in Table 2 (complete differential expression analyses are available in Supplementary Excel File S1).

As expected from previous RT-qPCR assays (Farhan UI Haque et al. 2015a; Gu et al. 2016), when comparing the transcriptome of *M. trichosporium* OB3b grown with 0 μM copper + 0 μM cerium vs. 0 μM copper + 25 μM cerium, genes encoding for the rare earth element-containing methanol dehydrogenase (Xox1- and Xox2-MeDH) increased in the presence of cerium. Interestingly, so did genes predicted to be involved in the synthesis and uptake of pyoverdine—a siderophore initially identified in *Pseudomonas* species for iron uptake (Wandersman and Delepelaire 2004). The only other genes significantly upregulated by cerium were one gene encoding for a σ^{70} factor (located in the pyoverdine gene cluster), two genes encoding for ABC transporters (one located in the pyoverdine gene cluster and the other located near the *xox2* gene cluster), and a gene encoding for protein of unknown function immediately upstream of *xoxF1* (Table 2; Supplementary Excel File S1).

Genes encoding for the calcium-containing methanol dehydrogenase (Mxa-MeDH) were downregulated in the

Table 1 Selected genes with annotated function that were differentially expressed in *M. trichosporium* OB3b when grown with 10 μM copper + 0 μM cerium vs. 0 μM copper + 0 μM cerium (Benjamini-Hochberg-adjusted p value < 1×10^{-3}, $|\log_2| > 1.5$). Note that complete differential expression analyses are available in the supplementary information as Supplementary Excel File S1

Function	Gene/locus number	p value	Log_2 fold change
Upregulated in 10 μM copper + 0 μM cerium compared with 0 μM copper + 0 μM cerium			
Particulate methane monooxygenase	*pmoA1* (ADVE02_v2_10400)	2.87E−08	2.27
	pmoA2 (ADVE02_v2_12979)	6.26E−10	2.49
	pmoB1 (ADVE02_v2_10399)	3.01E−10	2.52
	pmoB2 (ADVE02_v2_12980)	3.19E−08	2.26
Copper storage protein	*csp1* (ADVE02_v2_12455)	9.27E−17	2.38
Transporters	ABC-type (ADVE02_v2_12321)	1.98E−12	1.57
	modA (ADVE02_v2_12892)	2.14E−05	1.79
	cusA (ADVE02_v2_12040)	2.03E−36	4.46
	cusB (ADVE02_v2_12041)	9.91E−112	5.95
	Porin (ADVE02_v2_14468)	5.34E−04	2.19
Ribosomal proteins	*rplB* (ADVE02_v2_12932)	6.70E−04	2.65
	rplD (ADVE02_v2_12930)	6.76E−04	2.62
	rplE (ADVE02_v2_12941)	8.76E−04	2.58
	rplP (ADVE02_v2_12936)	2.94E−04	2.75
	rplV (ADVE02_v2_12934)	6.98E−04	2.60
	rplW (ADVE02_v2_12931)	3.72E−04	2.72
	rpmC (ADVE02_v2_12937)	6.21E−04	2.63
	rpsH (ADVE02_12943)	6.61E−04	2.58
	rpsN (ADVE02_12942)	7.09E−04	2.64
	rpsQ (ADVE02_12938)	9.69E−04	2.56
	rpsS (ADVE02_12933)	5.72E−04	2.64
Downregulated in 10 μM copper + 0 μM cerium compared with 0 μM copper + 0 μM cerium			
Soluble methane monooxygenase	*mmoB* (ADVE02_v2_12512)	5.62E−129	− 8.84
	mmoC (ADVE02_v2_12515)	1.22E−291	− 7.68
	mmoD (ADVE02_v2_12514)	0.00E+00	− 8.76
	mmoG (ADVE02_v2_12509)	8.75E−72	− 5.27
	mmoR (ADVE02_v2_12507)	3.88E−49	− 5.20
	mmoX (ADVE02_v2_12510)	0.00E+00	− 9.51
	mmoY (ADVE02_v2_12511)	9.91E−132	− 8.96
	mmoZ (ADVE02_v2_12513)	4.95E−158	− 9.05
Methanobactin synthesis and transport	*mbnA* (ADVE02_v2_13652)	3.36E−46	− 6.48
	mbnB (ADVE02_v2_13653)	6.74E−44	− 5.87
	mbnC (ADVE02_v2_13655)	1.08E−33	− 5.29
	mbnH (ADVE02_v2_13659)	4.67E−72	− 5.35
	mbnM (ADVE02_v2_13656)	3.29E−32	− 4.69
	mbnN (ADVE02_v2_13657)	6.56E−14	− 3.91
	mbnP (ADVE02_v2_13658)	2.06E−67	− 5.73
	mbnT (ADVE02_v2_13651)	1.30E−33	− 4.96
Transporters	ABC-type (ADVE02_v2_10934)	1.33E−04	− 1.98
	RND-type (ADVE02_v2_11413)	8.83E−08	− 1.57
	TonB-dependent (ADVE02_v2_10030)	3.81E−09	− 2.81
	(ADVE02_v2_10151)	5.86E−24	− 3.67
	(ADVE02_v2_11125)	7.80E−05	− 2.64
	(ADVE02_v2_11295)	2.97E−22	− 3.01
	(ADVE02_v2_11307)	8.90E−08	− 1.97

Table 1 (continued)

Function	Gene/locus number	*p* value	Log_2 fold change
	(ADVE02_v2_11588)	1.28E−21	− 5.12
	(ADVE02_v2_12266)	4.30E−10	− 2.05
	(ADVE02_v2_12284)	1.17E−08	− 1.76
	(ADVE02_v2_13641)	9.80E−12	− 2.10
	(ADVE02_v2_13988)	2.54E−22	− 2.14
	(ADVE02_v2_14392)	2.83E−15	− 3.05
	(ADVE02_v2_20043)	9.48E−07	− 1.79
Transcription regulators	FecRI-homologs (ADVE02_v2_10211)	2.73E−05	− 1.89
	(ADVE02_v2_10212)	4.85E−06	− 2.39
	(ADVE02_v2_11296)	2.46E−35	− 3.11
	(ADVE02_v2_11297)	4.28E−10	− 2.49
	(ADVE02_v2_11828)	7.74E−08	− 1.60
	(ADVE02_v2_13990)	1.19E−08	− 2.23
	(ADVE02_v2_14098)	4.48E−10	− 2.47
	(ADVE02_v2_14393)	5.54E−12	− 2.88
	(ADVE02_v2_14,394)	1.31E−09	− 3.24
	(ADVE02_v2_20042)	1.76E−06	− 1.61
	σ^{24} (ADVE02_v2_10149)	7.93E−04	− 1.81
	(ADVE02_v2_11305)	1.96E−04	− 1.66
	(ADVE02_v2_11827)	8.71E−05	− 1.75
	(ADVE02_v2_12264)	3.86E−11	− 2.41
	σ^{70} (ADVE02_v2_13661)	2.01E−88	− 5.11

presence of cerium (Table 2). Three genes encoding for either a TonB-dependent receptor, a pentapeptide repeat protein, and a protein of unknown function immediately upstream of *mxaF* were the only other genes to exhibit decreased expression when cerium was added in the absence of copper (Table 2; Supplementary Excel File S1).

Differentially expressed genes in the presence or absence of cerium and in the presence of copper

When comparing the transcriptome of *M. trichosporium* OB3b grown with 10 μM copper + 0 μM cerium vs. 10 μM copper + 25 μM cerium, only seven genes were upregulated when cerium was added in the presence of copper. Those with annotated function are listed in Table 3; complete differential analyses are shown in Supplementary Excel File S1. These included genes encoding for Xox1-MeDH, an ABC-type transporter, a TonB-dependent transporter, and an MxaD homolog that is believed to be involved in electron transfer between the methanol dehydrogenase and cytochrome c (Toyama et al. 2003). Thirty-six genes were found to be downregulated, most notably genes encoding for nitrogenase and hydrogenase as summarized in Table 3, as well as many genes encoding for proteins of unknown function (Supplementary Excel File S1).

Differentially expressed genes in the presence or absence of copper and in the presence of cerium

When comparing the transcriptome of *M. trichosporium* OB3b grown with 0 μM copper + 25 μM cerium or 10 μM copper + 25 μM cerium, over 780 genes, approximately 15% of the entire genome, were found to be either up- or downregulated. Figure 2 maps major shifts in gene expression for various metabolic pathways and uptake systems while Table 4 summarizes major changes in gene expression, i.e., genes involved in metal homeostasis, methane oxidation, transcriptional regulation, and cell synthesis are listed. Again, complete differential analyses are shown in Supplementary Excel File S1.

As found when copper was added in the absence of cerium (Table 1), if copper was added in the presence of cerium, genes involved in copper uptake decreased (*mbnA*) while those involved in copper efflux and storage increased (*cusAB* and *csp1*, respectively). Similarly, genes involved in pyoverdine synthesis decreased when copper was added in the presence of cerium.

Further, as found when comparing the transcriptomes of cultures grown with 0 μM copper + 0 μM cerium vs. 10 μM copper + 0 μM cerium, expression of genes encoding for 30S and 50S ribosomal proteins increased for cultures grown in the

Table 2 Genes with annotated function that were differentially expressed in *M. trichosporium* OB3b when grown with 0 μM copper + 25 μM cerium vs. 0 μM copper + 0 μM cerium (Benjamini-Hochberg-adjusted *p* value < 1×10^{-3}, $|\log_2| > 1.5$). Note that complete differential expression analyses are available in the supplementary information as Supplementary Excel File S1

Function	Gene/locus number	*p* value	Log_2 fold change
Upregulated in 0 μM copper + 25 μM cerium compared with 0 μM copper + 0 μM cerium			
Xox-type methanol dehydrogenase	*xoxF1* (ADVE02_v2_12117)	4.46E−30	3.89
	xoxF2 (ADVE02_v2_11799)	1.02E−05	2.50
	xoxG1 (ADVE02_v2_12118)	1.68E−18	2.48
	xoxG2 (ADVE02_v2_11797)	5.24E−11	2.93
	xoxJ2 (ADVE02_v2_11798)	2.00E−05	2.28
Pyoverdine synthesis and transport	*aphA* (ADVE02_v2_30012)	3.09E−08	2.06
	fpvA (ADVE02_v2_30019)	8.18E−09	2.37
	mbtH (ADVE02_v2_30032)	1.71E−27	5.11
	pvdA (ADVE02_v2_30015)	7.53E−18	3.03
	pvdF (ADVE02_v2_30013)	4.97E−25	3.54
	pvdH (ADVE02_v2_30016)	3.61E−15	2.81
	pvdL (ADVE02_v2_30029)	2.56E−07	1.74
ABC-type transporters	(ADVE02_v2_11792)	2.09E−05	2.42
	(ADVE02_v2_30018)	1.18E−06	1.78
σ^{70} transcription regulator	(ADVE02_v2_30017)	8.41E−07	1.85
Downregulated in 0 μM copper + 25 μM cerium compared with 0 μM copper + 0 μM cerium			
Mxa-type methanol dehydrogenase	*mxaA* (ADVE02_v2_12103)	4.93E−11	− 3.21
	mxaC (ADVE02_v2_12102)	6.91E−16	− 4.14
	mxaD (ADVE02_v2_12099)	2.31E−15	− 4.24
	mxaF (ADVE02_v2_12109)	1.34E−41	− 6.19
	mxaG (ADVE02_v2_12107)	7.95E−52	− 5.72
	mxaH (ADVE02_v2_12098)	6.50E−12	− 3.41
	mxaI (ADVE02_v2_12106)	4.71E−52	− 6.24
	mxaJ (ADVE02_v2_12108)	5.20E−74	− 6.04
	mxaK (ADVE02_v2_12101)	4.67E−12	− 3.36
	mxaL (ADVE02_v2_12100)	8.43E−15	− 4.10
	mxaR (ADVE02_v2_12105)	1.23E−64	− 6.12
	mxaS (ADVE02_v2_12104)	3.25E−32	− 5.29
TonB-dependent transporter	(ADVE02_v2_10208)	3.59E−33	− 2.79
Pentapeptide repeat protein	(ADVE02_v2_11208)	3.91E−15	−3.25

presence of 10 μM copper + 25 μM cerium vs. 0 μM copper + 25 μM cerium. In addition, expression of genes involved in the conversion of formaldehyde to biomass via the serine cycle and ethylmalonyl-CoA pathway were upregulated as were genes for amino acid, tRNA, fatty acid and cobalamin synthesis, amongst many others (Fig. 2, Table 4). In the presence of copper and cerium, Mxa-and Xox1-MeDH were both expressed, while expression of a gene encoding for a subunit of the NAD-linked formate dehydrogenase decreased. Expression of nitrogenase and hydrogenase genes also decreased when copper was added in the presence of cerium.

RT-qPCR confirmation of differential gene expression

To confirm RNA-Seq findings that genes encoding for alternative MMOs (sMMO vs. pMMO), MeDHs (Mxa-MeDH vs Xox-MeDH), metal uptake systems (methanobactin and pyoverdine) and nitrogenase varied in response to varied concentrations of copper or cerium, more focused and accurate RT-qPCR assays of the following genes were performed: *mmoX* and *pmoA* (sMMO and pMMO, respectively), *mxaF*, *xoxF1* and *xoxF2* (Mxa-MeDH and Xox-MeDH, respectively), *mbnA* (methanobactin), *pvdF* (pyoverdine), and *nifH* (nitrogenase). Three genes—*rrs* (16 s rRNA), *clpX*, (a subunit of a ClpX-ClpP ATP-dependent serine protease), and *yjg* (a permease of the YjgP/YjgQ family)—were used as internal references. These were chosen as *rrs* was found earlier to be appropriate (Farhan Ul Haque et al. 2015a, b; Gu et al. 2016; Kalidass et al. 2015), and expression of *clpX* and *yjg* were observed to be invariant under the growth conditions described examined here, i.e., $\log_2$ expression changes < 0.05 as determined via RNA-Seq. Figure 3 shows changes in gene

Table 3 Selected genes with annotated function that were differentially expressed in *M. trichosporium* OB3b when grown with 10 μM copper + 25 μM cerium vs. 10 μM copper + 0 μM cerium (Benjamini-Hochberg-adjusted *p* value $< 1 \times 10^{-3}$, $|\log_2| > 1.5$). Note that complete differential expression analyses are available in the supplementary information as Supplementary Excel File S1

Function	Gene/locus number	*p* value	Log_2 fold change
Upregulated genes in 10 μM copper + 25 μM cerium compared with 10 μM copper + 0 μM cerium			
Xox-type methanol dehydrogenase	*xoxF1* (ADVE02_v2_12117)	1.56E−24	3.55
	xoxG1 (ADVE02_v2_12118)	1.68E−27	3.02
Transporters	ABC-type (ADVE02_v2_11791)	9.87E−04	2.01
	TonB-dependent (ADVE02_v2_10208)	2.90E−15	1.91
MxaD homolog	(ADVE02_v2_13992)	1.68E−27	1.72
Downregulated genes in 10 μM copper + 25 μM cerium compared with 10 μM copper + 0 μM cerium			
Hydrogenase	*hupH* (ADVE02_v2_14422)	7.48E−04	− 2.57
	hyaB (ADVE02_v2_14428)	5.81E−05	− 3.15
	hyaC (ADVE02_v2_14427)	1.50E−04	− 3.05
Nitrogenase	*frxA* (ADVE02_v2_13288)	3.47E−04	− 1.55
	nifB (ADVE02_v2_13287)	7.48E−04	− 1.68
	nifE (ADVE02_v2_13306)	3.10E−04	− 2.63
	nifN (ADVE02_v2_13307)	6.30E−04	− 2.42
	nifU (ADVE02_v2_ 13315)	9.87E−04	− 2.45
	nifX (ADVE02_v2_13308)	6.19E−04	− 2.32

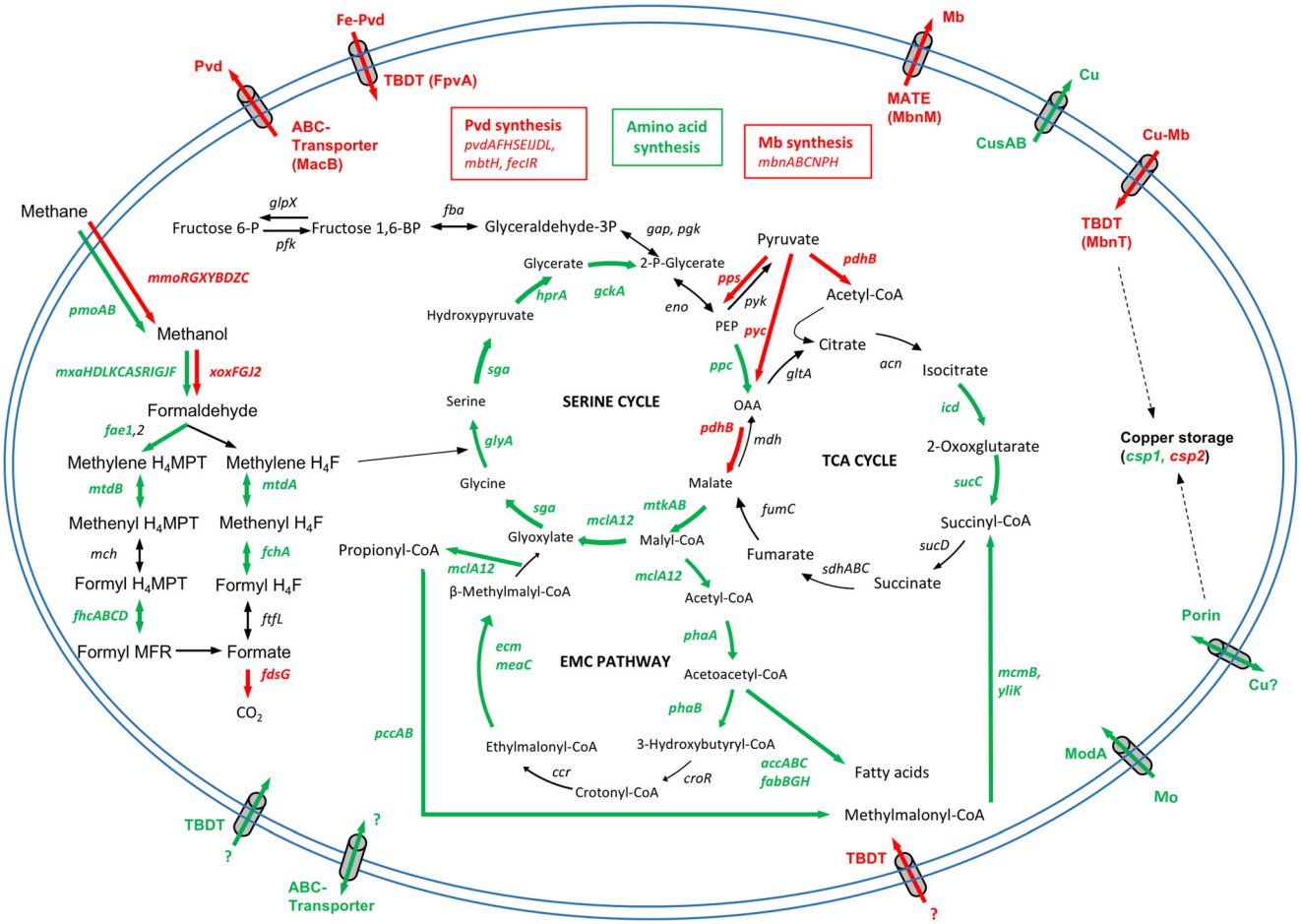

Fig. 2 Central metabolism of *M. trichosporium* OB3b. Genes highlighted in green or red were significantly upregulated or downregulated, respectively, when *M. trichosporium* OB3b was grown in the presence of 10 μM copper + 25 μM cerium vs. in the presence of 0 μM copper + 25 μM cerium. ABC-Transporter = ATP-binding cassette transporter, TBDT = TonB-dependent transporter, MATE = multi-antimicrobial extrusion protein, Mb = methanobactin, Pvd = pyoverdine

Table 4 Selected genes with annotated function that were differentially expressed in *M. trichosporium* OB3b when grown with 10 μM copper + 25 μM cerium vs. 0 μM copper + 25 μM cerium (Benjamini-Hochberg-adjusted p value < 1×10^{-3}, $|\log_2| > 1.5$). Note that complete differential expression analyses are available in the supplementary information as Supplementary Excel File S1

Function	Gene/locus number	p value	Log_2 fold change
Upregulated in 10 μM copper + 25 μM cerium vs. 0 μM copper + 25 μM cerium			
Particulate methane monooxygenase	*pmoA1* (ADVE02_v2_10400)	1.29E−07	2.11
	pmoA2 (ADVE02_v2_12979)	1.59E−07	2.10
	pmoB1 (ADVE02_v2_10399)	4.29E−05	1.64
	pmoB2 (ADVE02_v2_12980)	4.10E−05	1.64
Mxa-type methanol dehydrogenase	*mxaA* (ADVE02_v2_12103)	2.56E−19	4.12
	mxaC (ADVE02_v2_12102)	6.29E−28	5.37
	mxaD (ADVE02_v2_12099)	2.46E−27	5.53
	mxaF (ADVE02_v2_12109)	1.96E−42	6.19
	mxaG (ADVE02_v2_12107)	6.39E−64	6.30
	mxaH (ADVE02_v2_12098)	7.38E−22	4.50
	mxaI (ADVE02_v2_12106)	2.47E−54	6.33
	mxaJ (ADVE02_v2_12108)	1.43E−84	6.41
	mxaK (ADVE02_v2_12101)	4.34E−23	4.50
	mxaL (ADVE02_v2_12100)	1.90E−25	5.26
	mxaR (ADVE02_v2_12105)	6.47E−76	6.58
	mxaS (ADVE02_v2_12104)	4.95E−43	6.04
Formaldehyde oxidation	*fae1* (ADVE02_v2_12301)	3.14E−05	1.77
	fchA (ADVE02_v2_12564)	5.74E−06	2.19
	fhcA (ADVE02_v2_14361)	4.58E−06	2.19
	fhcB (ADVE02_v2_14362)	1.67E−05	1.73
	fhcC (ADVE02_v2_14359)	1.82E−06	2.43
	fhcD (ADVE02_v2_14360)	2.03E−06	2.36
	mtdA (ADVE02_v2_12565)	4.47E−06	2.42
	mtdB (ADVE02_v2_12229)	1.35E−04	1.94
Carbon assimilation	*ecm* (ADVE02_v2_10884)	8.61E−05	1.57
	gckA (ADVE02_v2_12558)	6.35E−05	1.91
	glyA (ADVE02_v2_13825)	1.38E−04	1.67
	hprA (ADVE02_v2_12566)	7.47E−05	2.10
	icd (ADVE02_v2_10351)	2.86E−04	1.55
	mclA1 (ADVE02_v2_12560)	2.61E−05	2.14
	mclA2 (ADVE02_v2_11719)	6.14E−05	1.77
	mcmB (ADVE02_v2_11451)	1.60E−05	2.05
	meaC (ADVE02_v2_14344)	4.38E−06	2.36
	mtkA (ADVE02_v2_12563)	1.57E−04	1.79
	mtkB (ADVE02_v2_12562)	7.82E−05	1.89
	pccA (ADVE02_v2_10751)	2.94E−06	2.11
	pccB (ADVE02_v2_11744)	2.06E−06	1.92
	phaA (ADVE02_v2_11388)	5.93E−06	1.71
	phaB (ADVE02_v2_11389)	5.57E−08	3.07
	ppc (ADVE02_v2_12561)	8.82E−06	2.35
	sga (ADVE02_v2_12567)	2.97E−06	2.74
	sucC (ADVE02_v2_11139)	3.32E−05	1.65
	yliK (ADVE02_v2_12495)	2.51E−06	1.65
Fatty acid synthesis	*accA* (ADVE02_v2_14271)	8.34E−04	1.52
	accB (ADVE02_v2_14116)	5.35E−07	1.96
	accC (ADVE02_v2_14117)	1.35E−09	2.84
	fabB (ADVE02_v2_13178)	7.20E−07	1.69
	fabG (ADVE02_v2_11402)	2.54E−05	1.89
	fabH1 (ADVE02_v2_11830)	2.34E−04	1.73
	fabH2 (ADVE02_v2_14383)	2.84E−05	1.87
Ribosomal proteins and rRNA maturation	*rimM* (ADVE02_v2_10846)	2.69E−05	2.32
	rlmJ (ADVE02_v2_10085)	3.11E−05	1.63

Table 4 (continued)

Function	Gene/locus number	*p* value	Log_2 fold change
	rplA (ADVE02_v2_12752)	5.87E−06	2.44
	rplB (ADVE02_v2_12932)	7.37E−08	3.73
	rplD (ADVE02_v2_12930)	1.15E−07	3.64
	rplE (ADVE02_v2_12941)	3.20E−08	3.80
	rplF (ADVE02_v2_12944)	4.96E−08	3.66
	rplI (ADVE02_v2_10233)	1.17E−06	2.21
	rplK (ADVE02_v2_12753)	1.63E−05	2.39
	rplL (ADVE02_v2_11490)	2.09E−04	1.97
	rplM (ADVE02_v2_10910)	8.65E−07	3.14
	rplN (ADVE02_v2_12939)	4.84E−08	3.71
	rplO (ADVE02_v2_12948)	3.34E−07	3.24
	rplP (ADVE02_v2_12936)	1.09E−08	3.91
	rplQ (ADVE02_v2_12500)	4.99E−06	2.28
	rplR (ADVE02_v2_12945)	1.26E−07	3.43
	rplT (ADVE02_v2_13716)	6.93E−06	2.27
	rplV (ADVE02_v2_12934)	2.37E−08	3.81
	rplW (ADVE02_v2_12931)	5.28E−08	3.74
	rplX (ADVE02_v2_12940)	4.72E−08	3.70
	rplY (ADVE02_v2_12131)	1.75E−04	2.02
	rpmC (ADVE02_v2_12937)	4.90E−08	3.74
	rpmD (ADVE02_v2_12947)	3.85E−07	3.32
	rpmH (ADVE02_v2_13333)	3.96E−06	1.52
	rpmI (ADVE02_v2_13717)	1.37E−05	2.14
	rpsB (ADVE02_2_11840)	6.71E−04	1.65
	rpsC (ADVE02_2_12935)	2.62E−06	3.42
	rpsD (ADVE02_2_11529)	4.12E−06	2.78
	rpsF (ADVE02_2_11513)	6.49E−04	1.96
	rpsH (ADVE02_2_12943)	3.57E−08	3.72
	rpsI (ADVE02_2_10909)	5.66E−08	3.61
	rpsK (ADVE02_2_12498)	2.70E−04	1.74
	rpsN (ADVE02_2_12942)	1.10E−07	3.68
	rpsO (ADVE02_2_10701)	2.69E−05	1.87
	rpsP (ADVE02_2_10845)	3.77E−06	2.63
	rpsQ (ADVE02_2_12938)	5.66E−08	3.73
	rpsS (ADVE02_2_12933)	4.68E−08	3.75
	rsmD (ADVE02_v2_13165)	1.17E−09	2.15
tRNA synthetase	*alaS* (ADVE02_v2_12800)	1.38E−04	1.50
	gatA (ADVE02_v2_10426)	5.06E−05	1.64
	hisS (ADVE02_v2_12393)	1.20E−04	1.61
	mtaB (ADVE02_v2_10603)	5.87E−06	1.53
	pheT (ADVE02_v2_11823)	1.82E−06	1.90
	queA (ADVE02_v2_10342)	1.64E−07	1.74
	thrS (ADVE02_v2_11769)	1.32E−05	1.90
	truB (ADVE02_v2_12786)	1.36E−06	2.09
	tsaD (ADVE02_v2_12701)	2.10E−05	1.57
	tyrS (ADVE02_v2_10186)	1.04E−04	1.51
	valS (ADVE02_v2_13325)	1.40E−05	1.91
Cellular division	*ftsE* (ADVE02_v2_10243)	5.58E−07	1.67
	ftsX (ADVE02_v2_10242)	1.27E−06	1.80
	parA (ADVE02_v2_12452)	1.90E−06	1.51
	parB (ADVE02_v2_12453)	9.97E−06	2.03
Amino acid synthetases	*argB* (ADVE02_v2_13329)	7.49E−05	1.79
	argF (ADVE02_v2_12391)	1.38E−06	2.23
	argH (ADVE02_v2_12625)	1.67E−04	1.86
	argJ (ADVE02_v2_12460)	6.15E−06	2.27

Table 4 (continued)

Function	Gene/locus number	*p* value	Log_2 fold change
	glnA (ADVE02_v2_10779)	1.19E−05	2.00
	hisA (ADVE02_v2_13556)	7.13E−06	1.77
	hisC (ADVE02_v2_13277)	2.84E−05	1.70
	hisG (ADVE02_v2_10098)	1.32E−04	1.72
	hisH (ADVE02_v2_13557)	7.59E−06	1.67
	ilvC (ADVE02_v2_13727)	5.19E−05	1.87
	leuB (ADVE02_v2_11144)	5.87E−06	2.28
	leuD (ADVE02_v2_12339)	2.05E−04	1.70
	proB (ADVE02_v2_10193)	5.27E−04	1.66
	serC (ADVE02_v2_12859)	2.87E−05	1.89
	thrB (ADVE02_v2_11436)	5.55E−08	1.96
	trpE (ADVE02_v2_10860)	5.19E−05	1.74
NADH-quinone oxidoreductase	*nuoB* (ADVE02_v2_14048)	4.25E−04	1.65
	nuoC (ADVE02_v2_14050)	5.90E−05	2.01
	nuoD (ADVE02_v2_14051)	4.48E−06	2.47
	nuoE (ADVE02_v2_14052)	7.33E−07	2.58
	nuoF (ADVE02_v2_14053)	1.81E−06	2.61
	nuoG (ADVE02_v2_14054)	3.97E−07	2.81
	nuoH (ADVE02_v2_14055)	1.04E−06	2.73
	nuoI (ADVE02_v2_14056)	1.97E−06	2.57
	nuoJ (ADVE02_v2_14057)	1.02E−07	2.84
	nuoK (ADVE02_v2_14058)	7.32E−08	2.98
	nuoL (ADVE02_v2_14059)	1.06E−07	2.93
	nuoM (ADVE02_v2_14060)	1.15E−07	2.92
	nuoN (ADVE02_v2_14061)	3.22E−08	2.88
Vitamin synthesis	*bioB* (ADVE02_v2_14107)	8.70E−07	1.77
	cobB (ADVE02_v2_13108)	4.96E−06	1.71
	cobD (ADVE02_v2_10145)	6.51E−06	2.16
	cobF (ADVE02_v2_13107)	1.62E−06	2.17
	cobH (ADVE02_v2_13115)	1.20E−04	1.87
	cobI (ADVE02_v2_13114)	4.02E−05	2.00
	cobJ (ADVE02_v2_13113)	6.13E−05	1.63
	cobL (ADVE02_v2_13111)	6.21E−06	2.27
	cobM (ADVE02_v2_13109)	5.29E−08	2.41
	cobN (ADVE02_v2_11366)	3.49E−07	2.52
	cobO (ADVE02_v2_11365)	5.66E−08	3.02
	cobQ (ADVE02_v2_10146)	6.72E−06	1.76
	cobT (ADVE02_v2_10147)	1.25E−06	2.21
	cobW (ADVE02_v2_11367)	5.69E−06	1.89
ATP synthase	*atpA* (ADVE02_v2_10591)	1.25E−06	2.79
	atpB (ADVE02_v2_10589)	1.71E−07	3.21
	atpB (ADVE02_v2_11080)	7.11E−04	1.82
	atpC (ADVE02_v2_10588)	2.29E−08	3.30
	atpE (ADVE02_v2_11079)	1.31E−06	2.62
	atpF1 (ADVE02_v2_11077)	1.62E−05	2.40
	atpF2 (ADVE02_v2_11078)	3.21E−05	2.21
	atpG (ADVE02_v2_10590)	2.73E−07	3.05
Transcription regulators	*oxyR* (ADVE02_v2_13066)	6.59E−05	1.90
	TetR-like (ADVE02_v2_12329)	2.72E−04	1.61
Copper storage protein	*csp1* (ADVE02_v2_12455)	2.93E−24	2.85
Flagella synthesis	(ADVE02_v2_11181)	3.36E−04	1.92
	(ADVE02_v2_11202)	1.56E−04	1.81
Transporters	ABC-type)		
	(ADVE02_v2_12321	6.34E−14	1.65
	(ADVE02_v2_12556)	7.89E−07	1.93

Table 4 (continued)

Function	Gene/locus number	*p* value	Log_2 fold change
	(ADVE02_v2_13887)	1.88E−07	1.87
	cusA (ADVE02_v2_12040)	1.68E−25	3.72
	cusB (ADVE02_v2_12041)	7.43E−95	5.48
	MATE-type (ADVE02_v2_10282)	6.89E−05	1.52
	modA (ADVE02_v2_12892)	1.13E−09	2.40
	Protein translocases		
	(ADVE02_v2_10024)	6.54E−07	2.45
	(ADVE02_v2_10025)	3.08E−06	2.24
	(ADVE02_v2_12441)	5.96E−06	2.14
	RND-type		
	(ADVE02_v2_11509)	1.25E−05	1.96
	(ADVE02_v2_11510)	2.93E−05	2.13
	(ADVE02_v2_11574)	3.97E−05	1.77
	TonB-dependent		
	(ADVE02_v2_10208)	3.24E−74	4.12
	(ADVE02_v2_10668)	1.39E−05	1.68
	(ADVE02_v2_13035)	3.01E−07	2.15
	(ADVE02_v2_14446)	7.98E−06	2.74
	(ADVE02_v2_14451)	3.37E−06	1.71
Downregulated in 10 μM copper + 25 μM cerium vs. 0 μM copper + 25 μM cerium			
Soluble methane monooxygenase	*mmoB* (ADVE02_v2_12512)	2.36E−137	− 9.12
	mmoC (ADVE02_v2_12515)	0.00E+00	− 8.14
	mmoD (ADVE02_v2_12514)	0.00E+00	− 9.15
	mmoG (ADVE02_v2_12509)	5.93E−72	− 5.26
	mmoR (ADVE02_v2_12507)	9.82E−50	− 5.21
	mmoX (ADVE02_v2_12510)	0.00E+00	− 10.00
	mmoY (ADVE02_v2_12511)	9.48E−141	− 9.26
	mmoZ (ADVE02_v2_12513)	1.54E−171	− 9.42
Xox-type methanol dehydrogenase	*xoxF2* (ADVE02_v2_11799)	2.93E−04	− 1.84
	xoxG2 (ADVE02_v2_11797)	7.79E−13	− 3.06
	xoxJ2 (ADVE02_v2_11798)	8.02E−09	− 2.75
Formate dehydrogenase	*fdsG* (ADVE02_v2_11629)	2.48E−07	− 1.68
Methanobactin synthesis and transport	*mbnA* (ADVE02_v2_13652)	3.87E−52	− 6.88
	mbnB (ADVE02_v2_13653)	2.68E−54	−6.52
	mbnC (ADVE02_v2_13655)	1.06E−39	− 5.73
	mbnH (ADVE02_v2_13659)	1.07E−80	− 5.65
	mbnM (ADVE02_v2_13656)	1.10E−33	− 4.78
	mbnN (ADVE02_v2_13657)	1.70E−15	− 4.10
	mbnP (ADVE02_v2_13658)	4.07E−77	− 6.12
	mbnT (ADVE02_v2_13651)	9.31E−26	− 4.33
Pyoverdine synthesis and transport	*fpvA* (ADVE02_v2_30019)	9.71E−12	− 2.64
	macB (ADVE02_v2_30010)	1.49E−09	− 1.66
	mbtH (ADVE02_v2_30032)	2.15E−32	− 4.86
	pvdA (ADVE02_v2_30015)	1.35E−30	− 3.87
	pvdF (ADVE02_v2_30013)	5.28E−41	− 4.45
	pvdH (ADVE02_v2_30016)	2.07E−26	− 3.58
	pvdL (ADVE02_v2_30029)	7.13E−14	− 2.29
Nitrogenase	*frxA* (ADVE02_v2_13288)	4.27E−07	− 1.85
	nifB (ADVE02_v2_13287)	7.85E−10	− 2.55
	nifD (ADVE02_v2_13304)	5.89E−04	− 2.06
	nifE (ADVE02_v2_13306)	1.89E−04	− 2.28
	nifH (ADVE02_v2_13303)	3.59E−04	− 2.18
	nifN (ADVE02_v2_13307)	5.26E−04	− 2.05
	nifU (ADVE02_v2_ 13,315)	1.33E−04	− 2.36
	nifW (ADVE02_v2_ 13,319)	8.93E−04	− 1.76

Table 4 (continued)

Function	Gene/locus number	*p* value	Log_2 fold change
	nifX (ADVE02_v2_ 13,308)	4.08E−04	− 2.00
Hydrogenase	*hupF* (ADVE02_v2_14424)	6.16E−04	− 2.13
	hupG (ADVE02_v2_14423)	4.04E−05	− 2.54
	hupH (ADVE02_v2_14422)	1.33E−04	− 2.43
	hupJ (ADVE02_v2_14420)	9.40E−04	− 2.14
	hyaA (ADVE02_v2_14429)	4.08E−06	− 2.95
	hyaB (ADVE02_v2_14428)	6.84E−05	− 2.65
	hyaC (ADVE02_v2_14427)	2.92E−04	− 2.44
	hyaD (ADVE02_v2_14426)	4.15E−04	− 2.21
	hybF (ADVE02_v2_14418)	1.64E−04	− 1.94
	hydA (ADVE02_v2_11109)	7.35E−04	− 1.72
	hypB (ADVE02_v2_14417)	6.88E−06	− 2.19
	hypC (ADVE02_v2_14415)	8.96E−04	− 1.73
	hypD (ADVE02_v2_14414)	9.12E−05	− 1.81
	hypF (ADVE02_v2_14416)	6.84E−05	− 1.96
	Nickel-dependent hydrogenase		
	(ADVE02_v2_10849)	1.11E−04	− 2.04
	(ADVE02_v2_10852)	5.92E−04	− 1.84
	(ADVE02_v2_10853)	7.65E−06	− 2.11
Copper storage protein	*csp2* (ADVE02_v2_10455)	9.26E−07	− 2.32
Transcription regulators	FecRI-homologs		
	(ADVE02_v2_10212)	9.68E−04	− 1.62
	(ADVE02_v2_11296)	9.88E−38	− 3.19
	(ADVE02_v2_11297)	1.58E−22	− 3.68
	(ADVE02_v2_13990)	6.10E−11	− 2.44
	(ADVE02_v2_14098)	1.36E−09	− 2.34
	(ADVE02_v2_14393)	9.06E−07	− 2.06
	fixJ (ADVE02_v2_11038)	1.54E−11	− 2.68
	LuxR-homolog		
	(ADVE02_v2_12868)	2.49E−07	− 1.69
	rpoH (ADVE02_v2_11218)	1.18E−07	− 3.37
	SigH-homolog (ADVE02_v2_10962)	1.30E−05	− 2.16
	TetR-homolog (ADVE02_v2_10058)		
	σ^{24}	1.12E−10	− 1.68
	(ADVE02_v2_11827)		
	(ADVE02_v2_12264)	8.52E−05	− 1.58
	(ADVE02_v2_ 14,394)	2.32E−09	− 2.15
	σ^{70}	5.90E−08	− 2.86
	(ADVE02_v2_13661)		
	(ADVE02_v2_30017)	2.81E−84	− 4.90
	ABC-type	2.79E−15	− 2.60
Transporters	(ADVE02_v2_12305)		
	(ADVE02_v2_30003)	2.91E−04	− 1.83
	(ADVE02_v2_30018)	1.22E−04	− 1.53
	(ADVE02_v2_30146)	1.02E−10	− 2.15
	actP (ADVE02_v2_14129)	1.64E−07	− 1.59
	MATE-type (ADVE02_v2_12268)	3.32E−05	− 1.70
	RND-type	1.54E−04	− 1.71
	(ADVE02_v2_11413)		
	(ADVE02_v2_30009)	3.06E−09	− 1.64
	TonB-dependent	5.58E−09	−2.12
	(ADVE02_v2_10030)		
	(ADVE02_v2_10151)	2.58E−05	− 1.98
	(ADVE02_v2_11295)	1.55E−42	− 4.86
	(ADVE02_v2_11307)	1.81E−24	− 3.14

Table 4 (continued)

Function	Gene/locus number	*p* value	Log_2 fold change
	(ADVE02_v2_11411)	2.71E−07	− 1.84
	(ADVE02_v2_11588)	1.42E−05	− 1.54
	(ADVE02_v2_12266)	1.17E−19	− 4.85
	(ADVE02_v2_12284)	8.00E−13	− 2.29
	(ADVE02_v2_12822)	3.13E−11	− 1.98
	(ADVE02_v2_13641)	1.81E−06	− 2.21
	(ADVE02_v2_13988)	1.95E−21	− 2.82
	(ADVE02_v2_14392)	1.42E−19	− 1.97
	(ADVE02_v2_20043)	5.70E−09	− 2.30

expression when the geometric mean of all three reference standards was used; similar trends were found when any one reference gene was used (Supplementary Figs. S2–S4).

As expected from RNA-Seq data, expression of *mmoX* and *mbnA* significantly decreased when copper was added, while *pmoA* expression increased, and such changes occurred regardless if cerium was present or not ($p < 0.05$; Fig. 3). Further, expression of *xoxF1* increased when cerium was added both in the absence and presence of copper while expression of *xoxF2* increased when cerium was added only in the absence of copper. *mxaF* expression only decreased when cerium was added in the absence of copper (Fig. 3, $p < 0.05$). *nifH* expression was also found to decrease in the presence of both copper and cerium as compared in the absence of both metals or in the presence of cerium only, i.e., there was no difference in *nifH* expression for *M. trichosporium* OB3b grown with 10 μM copper + 0 μM cerium and 10 μM copper + 25 μM cerium. Finally, *pvdF* was also found to be upregulated when cerium was added, but only in the absence of copper. Interestingly, RT-qPCR indicated that *pvdF* expression decreased slightly when copper was added (Fig. 3) but no significant changes were observed in the RNA-Seq data. Collectively, the RT-qPCR data support the RNA-Seq data in that copper and cerium differentially affected gene expression in *M. trichosporium* OB3b.

Discussion

An earlier study of the transcriptome of *M. trichosporium* OB3b grown in the presence of 9 μM copper found expression of many genes reported here, e.g., *pmo*, *nif*, *mxa*, and *pvd* genes (Matsen et al. 2013). That study was very informative in elucidating the metabolism of methanotrophs, and we extend that initial work to consider how the transcriptome of *M. trichosporium* OB3b varies in response to copper and cerium. These metals were chosen as it has been found that they control expression of key parts of methanotrophic metabolism, i.e., genes encoding for methane and methanol oxidation (Choi et al. 2003; Chu and Lidstrom 2016; Farhan Ul Haque et al. 2015a; Gu et al. 2016; Nielsen et al. 1996, 1997; Vu et al. 2016). Interestingly, copper and cerium affected the expression of other genes, but such control was strongly dependent on if both metals were present.

In the absence of cerium, copper affected expression of genes encoding for sMMO, pMMO, and methanobactin, as found earlier using more focused RT-qPCR assays (Farhan Ul Haque et al. 2015a; Gu et al. 2016; Semrau et al. 2013). Interestingly, although copper is an important component of methanotrophic metabolism, these microbes (like others) appear to carefully regulate the distribution and amount of copper in vivo (Braymer and Giedroc 2014; Le Brun 2014; Porcheron et al. 2013). That is, expression of *mbn* genes (responsible for methanobactin synthesis) decreased in the presence of copper while expression *csp1* and *cusAB* (encoding for a copper storage protein and a copper efflux system respectively) increased. Such data indicates that *M. trichosporium* OB3b actively controls copper homeostasis and that it has a complex, interconnected system whereby copper uptake, storage, and excretion pathways are tightly coupled to effectively utilize copper while minimizing its toxicity.

When cerium was varied in the absence of copper, expression of fewer genes was observed to vary as compared to when copper was varied in the absence of cerium, suggesting that cerium (and by extension other REEs) plays a less significant role in methanotrophic metabolism than copper. Most notably, genes encoding for Xox-MeDH increased in expression, while those encoding for Mxa-MeDH had lower expression when cerium was added in the absence of copper. The finding of increased expression of pyoverdine synthesis genes when cerium was added in the absence of copper, however, is novel. Typically, expression of metal uptake systems increase with decreasing metal availability (Baichoo and Helmann, 2002; Baichoo et al. 2002; Ratledge and Dover 2000), suggesting that pyoverdine synthesis increased when cerium was added as cerium may have affected iron uptake in the absence of copper. When cerium was added in the presence of copper, however, expression of genes encoding for pyoverdine synthesis did not change.

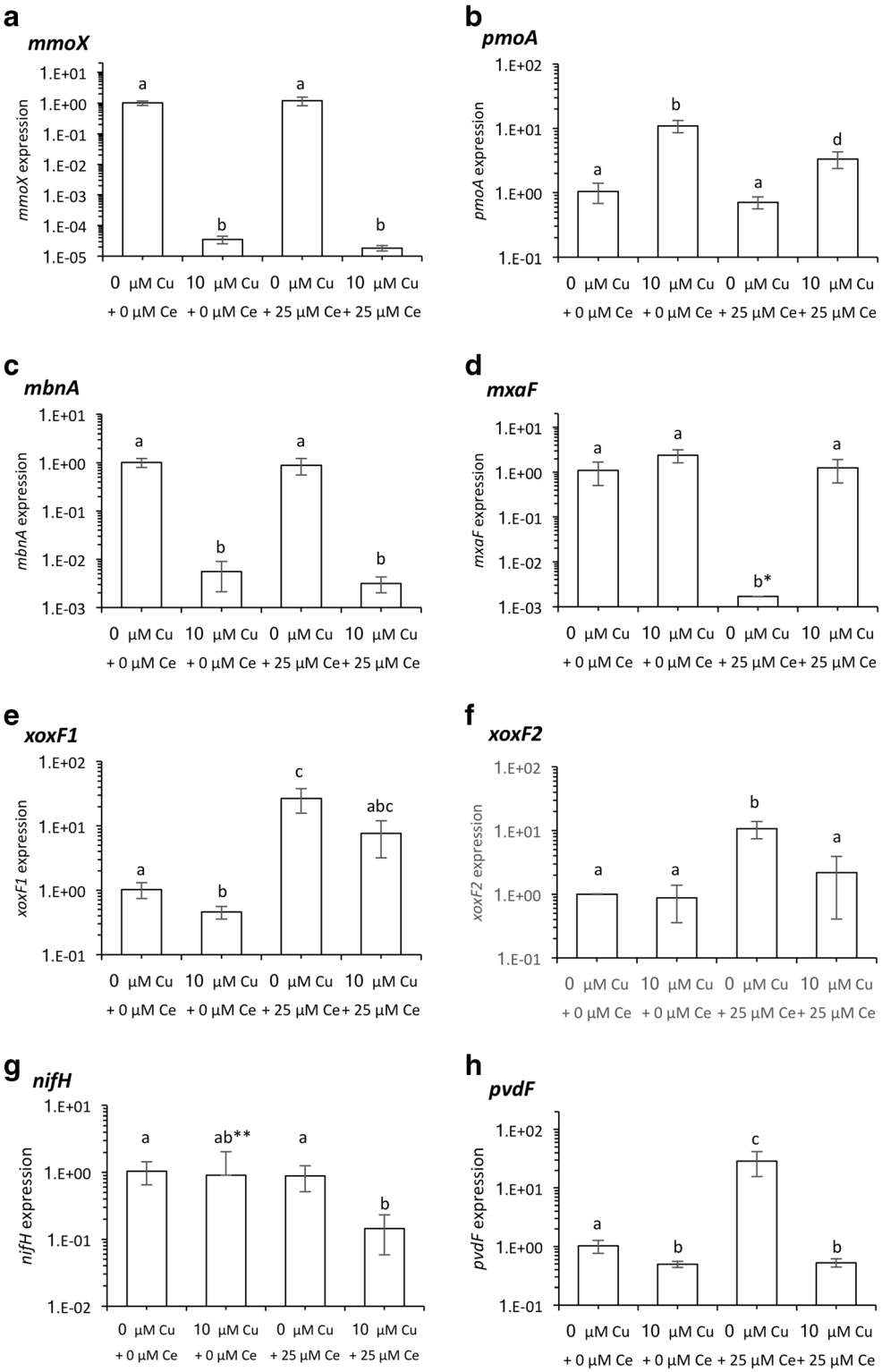

Fig. 3 RT-qPCR of selected genes using the geometric mean of the expression of *rrs* (16S rRNA), *clpX* (subunit of a ClpX-ClpP ATP-dependent serine protease), and *yjg* (YjgP/YjgO family permease) as an internal standard. **a** *mmoX* (α—subunit of sMMO hydroxylase). **b** *pmoA* (27-kDa polypeptide of pMMO). **c** *mbnA* (polypeptide precursor of methanobactin). **d** *mxaF* (66-kDa polypeptide of Mxa-MeDH). **e** *xoxF1* (65-kDa polypeptide of Xox1-MeDH). **f** *xoxF2* (65-kDa polypeptide of Xox2-MeDH). **g** *nifH* (dinitrogenase reductase subunit). **h** *pvdF* (responsible for synthesis of formyl hydroxamate groups in pyoverdine). Each bar represents average of triplicate cultures; error bars represent standard deviation. Bars within each plot labeled by different letters are significantly different ($p < 0.05$). Asterisk = error bars are too small to be visible. Double asterisk = lower error bar is too large to plot on the logarithmic scale

Quite unexpectedly, expression of nitrogenase decreased when copper and cerium were both added as compared to when only copper or cerium was present (Tables 3 and 4). Nitrogenase activity was not predicted under any condition as nitrate mineral salts (NMS) medium containing 9.9 mM NO_3^- was used for all cultures, and it has been shown that *M. trichosporium* OB3b has no N_2-fixation activity in this medium (Murrell and Dalton 1983). Others have shown, however, low expression of nitrogenase genes in *M. trichosporium* OB3b

when grown in NMS medium amended with copper (Matsen et al. 2013). Our data support these findings, and further indicate that nitrogenase expression is most affected when both copper and cerium are present, for reasons as yet unknown.

If copper was varied in the presence of cerium, expression of many genes was found to be affected (Fig. 2, Table 4). Under this condition, it again appears that copper homeostasis must be carefully managed given that, when copper was added in the presence of cerium, genes involved in copper uptake decreased (*mbnA*) while those involved in copper efflux and storage increased (*cusAB* and *csp1*, respectively). Further, genes for ATP synthase, ribosomal proteins, and many steps for the conversion of formaldehyde to biomass via the serine cycle and ethylmalonyl-CoA pathway were found to substantially increase when both copper and cerium were provided vs. cerium alone. In the presence of copper and cerium, Mxa-and Xox1-MeDH were both expressed, and as such, *M. trichosporium* OB3b may be converting methanol to formaldehyde more rapidly. In doing so, however, the cell must also increase the rate at which formaldehyde is transformed, either through oxidation to formate or assimilation into biomass, to control the buildup of this toxic intermediate. It is interesting to note that hydrogenase expression decreased in the presence of copper and cerium as compared to when cerium was only added (Table 4). It has been observed that several methanotrophs, including *M. trichosporium* OB3b, can generate significant amounts of H_2, with production dependent on the oxidation of formate to carbon dioxide (Hanczár et al. 2002; Kawamura et al. 1983). It appears H_2 generation is used to balance the ratio of NAD^+ to NADH by regenerating NAD^+ consumed during formate oxidation (Kawamura et al. 1983). It may be that in the presence of copper and cerium, carbon flux through the serine cycle and ethylmalonyl-CoA pathway increased to control the buildup of formaldehyde. In this scenario, carbon flow to carbon dioxide through formate would be reduced, decreasing the need to generate H_2 to balance NAD^+-NADH ratios. This speculation is supported (but not proven) by the finding of reduced expression of at least one gene encoding for a subunit of the NAD-linked formate dehydrogenase under these conditions (Fig. 2).

Alternatively, these hydrogenases may be used to consume hydrogen to consume H_2 generated from N_2 fixation. In this scenario, reduced hydrogenase expression in the presence of copper and cerium may be due to reduced nitrogenase expression. We must stress, however, that we cannot adequately explain reduced expression of either nitrogenase or hydrogenase in the presence of both copper and cerium with transcriptomic data alone. It would be interesting to examine the metabolome of *M. trichosporium* OB3b under varying amounts of copper and cerium, but such experiments are beyond the scope of this research.

In conclusion, we show herein that both copper and cerium affect the expression of many genes in *M. trichosporium* OB3b, but that the greatest changes occurred when both metals were present. Such studies may be very informative for manipulating methanotrophic metabolism for the valorization of methane. There is still much to be learned, however, about the role of copper and rare earth elements in methanotrophy, and it is difficult to overstate the importance of these metals in the metabolism of these microbes.

Funding This research was supported by the Office of Science (Biological and Environmental Research), US Department of Energy, Grant No. DE-SC0006630. The funder had no role in the study design, data collection, and interpretation, or the decision to submit the work for publication.

Compliance with ethical standards

Conflict of interest The authors declare that they have no conflict of interest.

Ethical approval This article does not contain any studies with human participants or animals performed by any of the authors.

References

Anders S, Huber W (2010) Differential expression analysis for sequence count data. Genome Biol 11:1

Anders S, Pyl PT, Huber W (2015) HTSeq–a Python framework to work with high-throughput sequencing data. Bioinformatics 31:166–169

Andrews S (2010) FastQC: a quality control tool for high throughput sequence data. http://www.bioinformatics.babraham.ac.uk/projects/fastqc. Accessed 1 August, 2016

Anthony CP, Williams P (2003) The structure and mechanism of methanol dehydrogenase. Biochim Biophys Acta 1647:18–23

Baichoo N, Helmann JD (2002) Recognition of DNA by Fur: a reinterpretation of the Fur box consensus sequence. J Bacteriol 184:5826–5832

Baichoo N, Wang T, Ye R, Helmann JD (2002) Global analysis of the *Bacillus subtilis* Fur regulon and the iron starvation stimulon. Mol Microbiol 45:1613–1629

Braymer JJ, Giedroc DP (2014) Recent developments in copper and zinc homeostasis in bacterial pathogens. Curr Opin Chem Biol 19:59–66

Choi DW, Kunz RC, Boyd ES, Semrau JD, Antholine WE, Han JI, Zahn JA, Boyd JM, Arlene M, DiSpirito AA (2003) The membrane-associated methane monooxygenase (pMMO) and pMMO-NADH:quinone oxidoreductase complex from *Methylococcus capsulatus* Bath. J Bacteriol 185:5755–5764

Chu F, Lidstrom ME (2016) XoxF acts as the predominant methanol dehydrogenase in the type I methanotroph *Methylomicrobium buryatense*. J Bacteriol 198:1317–1325

DiSpirito AA, Zahn JA, Graham DW, Kim HJ, Larive CK, Derrick TS, Cox CD, Taylor A (1998) Copper-binding compounds from *Methylosinus trichosporium* OB3b. J Bacteriol 180:3606–3613

DiSpirito AA, Semrau JD, Murrell JC, Gallagher WH, Dennison C, Vuilleumier S (2016) Methanobactin and the link between copper and bacterial methane oxidation. Microbiol Mol Biol Rev 80:387–409

Farhan Ul Haque M, Kalidass B, Bandow N, Turpin EA, DiSpirito AA, Semrau JD (2015a) Cerium regulates expression of alternative

methanol dehydrogenases in *Methylosinus trichosporium* OB3b. Appl Environ Microbiol 81:7546–7552

Farhan Ul Haque M, Kalidass B, Vorobev A, Baral BS, DiSpirito AA, Semrau JD (2015b) Methanobactin from *Methylocystis* strain SB2 affects gene expression and methane monooxygenase activity in *Methylosinus trichosporium* OB3b. Appl Environ Microbiol 81: 2466–2473

Goodwin PM, Anthony C (1998) The biochemistry, physiology and genetics of PQQ and PQQ-containing enzymes. Adv Microbial Physiol 40:1–80

Gu W, Farhan Ul Haque M, DiSpirito AA, Semrau JD (2016) Uptake and effect of rare earth elements on gene expression in *Methylosinus trichosporium* OB3b. FEMS Microbiol Lett 363:1–6

Hanczár T, Csáki R, Bodrossy L, Murrell JC, Kovács KL (2002) Detection and localization of two hydrogenases in *Methylococcus capsulatus* (Bath) and their potential role in methane metabolism. Arch Microbiol 177:167–172

Hanson RS, Hanson TE (1996) Methanotrophic bacteria. Microbiol Rev 60:439–471

Hibi Y, Asai K, Arafuka H, Hamajima M, Iwama T, Kawai K (2011) Molecular structure of La^{3+}-induced methanol dehydrogenase-like protein in *Methylobacterium radiotolerans*. J Biosci Bioeng 111: 547–549

Joshi NA, Fass JN (2011) Sickle: A sliding-window, adaptive, quality-based trimming tool for FastQ files. https://github.com/najoshi/sickle. Accessed 1 August 2016

Kalidass B, Farhan Ul Haque M, Baral BS, DiSpirito AA, Semrau JD (2015) Competition between metals for binding to methanobactin enables expression of soluble methane monooxygenase in the presence of copper. Appl Environ Microbiol 81:1024–1031

Kalyuzhnaya MG, Puri AW, Lidstrom ME (2015) Metabolic engineering in methanotrophic bacteria. Metab Engin 29:142–152

Kawamura S, O'Neil JG, Wilkinson JF (1983) Hydrogen production by methylotrophs under anaerobic conditions. J Ferment Technol 61: 151–156

Keltjens JT, Pol A, Reimann J, Op den Camp HJM (2014) PQQ-dependent methanol dehydrogenases: rare-earth elements make a difference. Appl Microbiol Biotechnol 98:6163–6183

Khmelenina VN, Rozova ON, But SY, Mustakhimov II, Reshetnikov AS, Beschastnyl AP, Trotsenko YA (2015) Biosynthesis of secondary metabolites in methanotrophs: biochemical and genetic aspects. Appl Biochem Microbiol 51:150–158

Langmead B, Salzberg S (2012) Fast gapped-read alignment with Bowtie 2. Nat Methods 9(4):357–359

Law CW, Chen Y, Shi W, Smyth GK (2014) Voom: precision weights unlock linear model analysis tools for RNA-Seq read counts. Genome Biol 15:1

Le Brun NE (2014) Copper in prokaryotes. In: Mert J, Wedd A (eds) RSC Metallobiology Series No. 2. Binding, transport and storage of metal ions in biological cells. Royal Society of Chemistry, London, pp 461–499

Lee SW, Keeney DR, Lim DH, DiSpirito AA, Semrau JD (2006) Mixed pollutant degradation by *Methylosinus trichosporium* OB3b expressing either soluble or particulate methane monooxygenase: can the tortoise beat the hare? Appl Environ Microbiol 72:7503–7509

Li H, Durbin R (2009) Fast and accurate short read alignment with Burrows-Wheeler transform. Bioinformatics 25:1760

Li H, Handsaker B, Wysoker A, Fennell T, Ruan J, Homer N, Marth G, Abecasis G, Durbin R (2009) 1000 genome project data processing subgroup. The sequence alignment/map (SAM) format and SAMtools. Bioinformatics 25:2079

Matsen J, Yang S, Stein LY, Beck D, Kalyuzhnaya MG (2013) Global molecular analyses of methane metabolism in methanotrophic alphaproteobacterium, *Methylosinus trichosporium* OB3b. Part I: transcriptomic study. Front Microbiol 4:40

Munson GP, Lam DL, Outten FW, O'Halloran TV (2000) Identification of a copper-responsive two component system on the chromosome of *Escherichia coli* K-12. J Bacteriol 182:5864–5871

Murrell JC, Dalton H (1983) Nitrogen fixation in obligate methanotrophs. J Gen Microbiol 129:3481–3496

Nakagawa T, Mitsui R, Tutani A, Sasa K, Tashiro S, Iwama T, Hayakawa T, Kawai K (2012) A catalytic role of XoxF1 as La^{3+}-dependent methanol dehydrogenase in *Methylobacterium extorquens* strain AM1. PLoS One 7:e50480

Nielsen AK, Gerdes K, Degn H, Murrell JC (1996) Regulation of bacterial methane oxidation: transcription of the soluble methane monooxygenase operon of *Methylococcus capsulatus* (Bath) is repressed by copper ions. Microbiology 142:1289–1296

Nielsen AK, Gerdes K, Murrell JC (1997) Copper-dependent reciprocal transcriptional regulation of methane monooxygenase genes in *Methylococcus capsulatus* and *Methylosinus trichosporium*. Molec Microbiol 25:399–409

Op den Camp HJM, Islam T, Stott MB, Harhangi HR, Hynes A, Schouten S, Jetten MS, Birkeland NK, Pol A, Dunfield PF (2009) Environmental, genomic and taxonomic perspectives on methanotrophic *Verrucomicrobia*. Environ Microbiol Reports 1:293–306

Pol A, Barends TRM, Dietl A, Khadem AF, Eygensteyn J, Jetten MSM, Op den Camp HJM (2014) Rare earth metals are essential for methanotrophic life in volcanic mudpots. Environ Microbiol 16: 255–264

Porcheron G, Garénaux A, Proulx J, Sabri M, Dozois CM (2013) Iron, copper, zinc, and manganese transport and regulation in pathogenic Enterobacteria: correlations between strains, site of infection, and the relative importance of the different metal transport systems for virulence. Front Cell Infection Microbiol 3:90

Ratledge C, Dover LG (2000) Iron metabolism in pathogenic bacteria. Annu Rev Microbiol 54:881–941

Schmidt S, Christen P, Kiefer P, Voholt JA (2010) Functional investigation of methanol dehydrogenase-like protein XoxF in *Methylobacterium extorquens* AM1. Microbiology 156:2575–2586

Schmittgen TD, Livak KJ (2008) Analyzing real-time PCR data by the comparative CT method. Nat Protoc 3:1101–1108

Semrau JD, DiSpirito AA, Yoon S (2010) Methanotrophs and copper. FEMS Microbiol Rev 34:496–531

Semrau JD, Jagadevan S, DiSpirito AA, Khalifa A, Scanlan J, Bergman BH, Freemeier BC, Baral BS, Bandow NL, Vorobev A, Haft DH (2013) Methanobactin and MmoD work in concert to act as the 'copper-switch' in methanotrophs. Environ Microbiol 15:3077–3086

Skovran E, Palmer AD, Rountree AM, Good NM, Lidstrom ME (2011) XoxF is required for expression of methanol dehydrogenase in *Methylobacterium extorquens* AM1. J Bacteriol 193:6032–6038

Stanley SH, Prior SD, Leak DJ, Dalton H (1983) Copper stress underlies the fundamental change in intracellular location of the methane monooxygenase in methane-oxidizing organisms: studies in batch and continuous cultures. Biotechnol Lett 5:487–492

Strong PJ, Xie S, Clarke WP (2015) Methane as a resource: can the methanotrophs add value? Environ Sci Technol 49:4001–4008

Toyama H, Inagaki H, Matsushita K, Anthony C, Adachi O (2003) The role of the MxaD protein in the respiratory chain of *Methylobacterium extorquens* during growth on methanol. Biochim Biophys Acta 1647:372–375

Trotsenko YA, Murrell JC (2008) Metabolic aspects of aerobic obligate methanotrophy. Adv Appl Microbiol 63:183–229

Vekeman B, Speth D, Wille J, Cremers G, De Vos P, Op den Camp HJM, Heylen K (2016) Genome characteristics of two novel type I methanotrophs enriched from North Sea sediments containing exclusively a lanthanide-dependent XoxF5-type methanol dehydrogenase. Microb Ecol 72:503–509

Vita N, Plataski S, Baslé A, Allen SJ, Paterson NG, Crombie AT, Murrell JC, Waldron KJ, Dennison C (2016) A four-helix bundle stores copper for methane oxidation. Nature 525:140–143

Vu HN, Subuyi GA, Vijayakumar S, Good NM, Martinez-Gomez NC, Skovran E (2016) Lanthanide-dependent regulation of methanol oxidation systems in *Methylobacterium extorquens* AM1 and their contribution to methanol growth. J Bacteriol 198:1250–1259

Wandersman C, Delepelaire P (2004) Bacterial iron sources: from siderophores to hemophores. Annu Rev Microbiol 58:611–647

Wehrmann M, Billard P, Martin-Meriadec A, Zegeye A, Klebensberger J (2017) Functional role of lanthanides in enzymatic activity and transcriptional regulation of pyrroloquinolone quinone-dependent alcohol dehydrogenases in *Pseudomonas putida* KT2440. MBio 8: E00570–E00517

Whittenbury R, Phillips KC, Wilkinson JF (1970) Enrichment, isolation and some properties of methane-utilizing bacteria. Microbiology 61: 205–218

Williams PA, Coates L, Mohammed F, Gill R, Erskine PT, Coker A, Wood SP, Anthony C, Cooper JB (2005) The atomic resolution structure of methanol dehydrogenase from *Methylobacterium extorquens*. Acta Crystal Sect D: Biol Crystal 61:75–79

Wu ML, Wessels HJ, Pol A, Op den Camp HJM, Jetten MSM, van Niftrik L, Keltjens JT (2015) XoxF-type methanol dehydrogenase from the anaerobic methanotroph "*Candidatus* Methylomirabilis oxyfera". Appl Environ Microbiol 81:1442–1451

Yoon S, Carey JN, Semrau JD (2009) Feasibility of atmospheric methane removal using methanotrophic biotrickling filters. Appl Microbiol Biotechnol 83:949–956